Consideration of thermal Hall effect in undoped cuprates

Jung Hoon Han,[1,*] Jin-Hong Park,[1] and Patrick A. Lee[2,†]

[1]*Department of Physics, Sungkyunkwan University, Suwon 16419, Korea*

[2]*Department of Physics, Massachusetts Institute of Technology, Cambridge, Massachusetts 02139, USA*

(Received 19 March 2019; revised manuscript received 10 May 2019; published 30 May 2019)

A recent observation of the thermal Hall effect of magnetic origin in underdoped cuprates calls for critical reexamination of low-energy magnetic dynamics in an undoped antiferromagnetic compound on square lattice, where traditional, renormalized spin-wave theory was believed to work well. Using the Holstein-Primakoff boson formalism, we find that magnon-based theories can lead to finite Berry curvature in the magnon band once the Dzyaloshinskii-Moriya spin interaction is taken into account explicitly, but fail to produce nonzero thermal Hall conductivity. Assuming accidental doping by impurities and magnon scattering off of such impurity sites fails to predict skew scattering at the level of the Born approximation. Local formation of skyrmion defects is also found incapable of generating the magnon thermal Hall effect. Turning to a spinon-based scenario, we write down a simple model by adding spin-dependent diagonal hopping to the well-known π-flux model of spinons. The resulting two-band model has a Chern number in the band structure, and generates thermal Hall conductivity whose magnetic field and temperature dependencies mimic closely the observed thermal Hall signals. In disclaimer, there is no firm microscopic basis of this model and we do not claim to have found an explanation of the data, but given the unexpected nature of the experimental observation, it is hoped this work could serve as a step towards reaching some level of understanding.

DOI: 10.1103/PhysRevB.99.205157

I. INTRODUCTION

Traditional views on the Hall effect have undergone dramatic changes over the past several decades, most prominently thanks to the observation of the quantized Hall effect in two-dimensional electronic systems and the subsequent realization that it is the band topology, rather than the magnetic field itself, that determines the Hall response of electronic systems [1,2]. It has become manifest over the years, both theoretically and experimentally, that even nonelectronic systems support Hall-like transport of their elementary excitations such as photons [3], phonons [4,5], magnons [6–15], and triplons [16] due to the topological character in their respective band structures or the emergent magnetic field governing their dynamics. More recently, there is growing experimental evidence of Hall-like heat (thermal) transport in magnetic materials that remain in paramagnetic, spin-liquid-like phases [17–21]. The physical picture regarding the origin of Hall-like phenomena for such correlated paramagnetic insulators remains poorly understood, as the Berry curvature effect only pertains to the band picture of weakly interacting quasiparticles. The Schwinger-boson mean-field approximation was introduced in Refs. [21,22] as a way to partly address the Hall effect in the paramagnetic phase. Magnetic materials exhibiting the thermal Hall effect are typically frustrated, with the pyrochlore or the kagome lattice structure [7,8,17–21] responsible for the geometric frustration, or possess a significant amount of Kitaev-type interaction leading to the emergence of novel Majorana excitation [20].

With this background, the recent observation of significant thermal Hall signal in the family of cuprate compounds comes as a surprise [23]. A few salient features of the experiment may be summed up. First, the undoped antiferromagnetically ordered compound La_2CuO_4 exhibits large thermal Hall conductivity κ_{xy} in the absence of electronic charge carriers. A phonon-related origin of κ_{xy} is ruled out, on the grounds that the spin-phonon scattering seems too weak to account for the large κ_{xx} value in the cuprates and that the weak (strong) magnetic field dependence of the longitudinal (transverse) thermal conductivity κ_{xx} (κ_{xy}) seems at odd with the phonon scenario. Furthermore, κ_{xy} is reduced in magnitude as doping increases and even undergoes a sign change at some finite temperature, reflecting a mixed contribution of electronic and magnetic origins upon doping. For underdoped (and presumably undoped) $La_{2-x}Sr_xCuO_4$, the Hall effect is almost linear in the applied magnetic field B. Magnons, on the other hand, must have an energy gap increasing with B and lead to the suppressed Hall effect at a larger B field. A general picture thus emerging is that the underdoped antiferromagnetic compound might have some nontrivial magnetic correlations, which are presumably gapless and revealed by the applied magnetic field through the transverse heat conduction.

What are the quasiparticles responsible for the observed transverse heat conductivity? First of all, the magnon in the experimental system has a sizable gap [23]. Second, even assuming this gap to be small, we expect the gap to grow with a magnetic field, whereas the thermal Hall effect initially increases with an applied field. There are other objections arising from purely theoretical consideration, such as the "no-go"

*hanjemme@gmail.com

†palee@mit.edu

theorem [6], disfavoring the formation of the topological Hall effect in unfrustrated square-lattice magnets. A way round this "theorem" was invented recently [24], by adopting a model complicated enough to break spatial symmetries of the square lattice; such models do not seem to apply readily to cuprates, though. Despite these objections, we categorically look into the magnon-based scenario and add various tweaks to it, with the hope that one such model might capture the thermal Hall phenomenology. In conclusion, as we report in Secs. II and III, the answer is negative; hardly any magnon-based scenario is likely to account for the thermal Hall effect in the square-lattice antiferromagnet. In Sec. IV we outline a completely different scenario based on the spinon picture of magnetic excitation. Treating spin excitations in terms of fractionalized fermions known as spinons is an old idea, dating back to Anderson's resonating valence bond proposal. The task of applying the spinon idea to work out magnetic excitations in the cuprates was taken up in the past, notably in Refs. [25,26]. We show that a small modification of this spinon model, built around the so-called π-flux phase and its Dirac-like dispersion, can lead to finite thermal Hall conductivity with temperature and magnetic field dependencies similar to the those observed [23]. We emphasize that the goal of our exercise is to find a model which is capable of producing thermal Hall conductivity of the size seen by experiment. One important requirement of such model would be that the effect is linear in the applied magnetic field, as seen in the data [23]; this is a feature quite naturally embodied in our model. Nevertheless, we do not claim to understand how this model can describe the cuprates. In particular we do not know how it can coexist with Néel ordering in the insulator. We feel, however, that the experimental results are so unexpected that our modest goal can hopefully be the first step towards an explanation.

Inspired by the same experiment, a recent preprint [27] also discussed the thermal conductivity in a spinon model, but they chose the bosonic spinon and as such their treatment is complementary to our fermionic spinon model. A number of their models explicitly break time-reversal symmetry and have net spin chirality spontaneously generated. These models will not have the thermal Hall effect that is linear in the magnetic field and generally speaking hysteresis may be expected.

II. MAGNON THEORY OF THERMAL HALL EFFECT IN SQUARE-LATTICE ANTIFERROMAGNETS

We begin by (re)visiting the well-known microscopic $S = 1/2$ spin Hamiltonian of the cuprates:

$$H = J\sum_{\langle ij\rangle} \mathbf{S}_i\cdot\mathbf{S}_j + \sum_{\langle ij\rangle}\mathbf{D}_{ij}\cdot\mathbf{S}_i\times\mathbf{S}_j - \mathbf{B}\cdot\sum_i \mathbf{S}_i. \tag{2.1}$$

In addition to the familiar spin exchange J, we allow the Dzyaloshinskii-Moriya (DM) interaction, originating from the small buckling of the oxygen atom out of the CuO_2 plane [28,29], and the Zeeman interaction. Sites on the square lattice are denoted simply by i and j, with $\langle ij\rangle$ indicating the nearest-neighbor pair of sites. The DM vectors as dictated by symmetry consideration were first worked out by Coffey *et al.* [30]:

$$\begin{aligned}\mathbf{D}_{i,i+\hat{x}} &= \sqrt{2}D(-1)^i(\cos\theta_d, \sin\theta_d),\\ \mathbf{D}_{i,i+\hat{y}} &= -\sqrt{2}D(-1)^i(\sin\theta_d, \cos\theta_d, 0).\end{aligned} \tag{2.2}$$

The factor $(-1)^i = (-1)^{i_x+i_y}$ keeps track of the staggering of the DM vector. The ordered spins are forced to lie in the CuO_2 plane due to the DM interaction, with a small out-of-plane ferromagnetic component also dictated by the same interaction. The mean-field ansatz can be chosen as

$$\langle\mathbf{S}_i\rangle = \mathbf{n}_i = n_0\hat{z} - n_1(-1)^i\hat{a}. \tag{2.3}$$

It proves convenient to work with a new pair of orthonormal axes $\hat{a} = (1, 1)/\sqrt{2}$ and $\hat{b} = (-1, 1)/\sqrt{2}$ instead of $\hat{x}$ and $\hat{y}$ axes which extend along Cu-Cu directions. An orthonormal triad is formed by $\hat{a}\times\hat{b} = \hat{z}$. The mean-field energy comes out as

$$E = 2J\left(n_0^2 - n_1^2\right) - 4D(\cos\theta_d - \sin\theta_d)n_0n_1 - Bn_0. \tag{2.4}$$

The Zeeman energy scale at $B = 10$ T is only a meV, whereas the DM energy may be several meV in the cuprates. As a result, the canting angle θ_c defined as $(n_0, n_1) = (\sin\theta_c, \cos\theta_c)$ is dictated by the ratio D/J, and not so much by the Zeeman field. Minimizing the energy E with respect to the canting angle θ_c gives

$$\tan 2\theta_c = (D/J)(\cos\theta_d - \sin\theta_d) \tag{2.5}$$

at $B = 0$. The sign of the DM energy D and the angle θ_d are chosen in such a way that the canting angle is positive, $\theta_c > 0$.

Next we introduce a general formalism that allows one to convert the spin Hamiltonian (2.1) to a magnon Hamiltonian, defined around a mean-field ground state given in Eq. (2.3). In doing so, we aim to see if the magnon theory or some of its variants can account for the thermal Hall phenomena in the undoped square-lattice antiferromagnet. The method is based on parametrizing the spin operator $\mathbf{S}_i$ as

$$\mathbf{S}_i = a_i\mathbf{n}_i + \mathbf{t}_i, \tag{2.6}$$

where a_i refers to the amplitude reduction along the direction of the classical ground-state spin $\mathbf{n}_i$, due to the transverse fluctuation $\mathbf{t}_i$. The well-known Holstein-Primakoff (HP) substitution follows from the formula

$$a_i = S - b_i^\dagger b_i,\ \ \mathbf{t}_i = t_i^\theta\boldsymbol{\theta}_i + t_i^\phi\boldsymbol{\phi}_i, \tag{2.7}$$

where

$$t_i^\theta = \sqrt{\frac{S}{2}}(b_i^\dagger + b_i),\ \ t_i^\phi = i\sqrt{\frac{S}{2}}(b_i^\dagger - b_i), \tag{2.8}$$

and $\boldsymbol{\theta}_i$ and $\boldsymbol{\phi}_i$ are a pair of orthonormal vectors forming the local triad $\boldsymbol{\theta}_i\times\boldsymbol{\phi}_i = \mathbf{n}_i$. For this choice of triad we are guaranteed the transversality condition $\mathbf{t}_i\cdot\mathbf{n}_i = 0$.

Substituting Eq. (2.6) and the rest of the HP formulas into the spin Hamiltonian gives the following magnon Hamiltonian:

$$\begin{aligned}H = &\sum_{\langle ij\rangle}[J\boldsymbol{\theta}_i\cdot\boldsymbol{\theta}_j + \mathbf{D}_{ij}\cdot\boldsymbol{\theta}_i\times\boldsymbol{\theta}_j]t_i^\theta t_j^\theta\\ &+ \sum_{\langle ij\rangle}[J\boldsymbol{\phi}_i\cdot\boldsymbol{\phi}_j + \mathbf{D}_{ij}\cdot\boldsymbol{\phi}_i\times\boldsymbol{\phi}_j]t_i^\phi t_j^\phi\end{aligned}$$

$$+\sum_{\langle ij\rangle}[J\boldsymbol{\theta}_i\cdot\boldsymbol{\phi}_j+\mathbf{D}_{ij}\cdot\boldsymbol{\theta}_i\times\boldsymbol{\phi}_j]t_i^\theta t_j^\phi$$
$$+\sum_{\langle ij\rangle}[J\boldsymbol{\phi}_i\cdot\boldsymbol{\theta}_j+\mathbf{D}_{ij}\cdot\boldsymbol{\phi}_i\times\boldsymbol{\theta}_j]t_i^\phi t_j^\theta-\sum_i\mu_i b_i^\dagger b_i, \tag{2.9}$$

where $\mu_i=J\sum_{j\in i}\mathbf{n}_i\cdot\mathbf{n}_j+\sum_{j\in i}\mathbf{D}_{ij}\cdot\mathbf{n}_i\times\mathbf{n}_j-\mathbf{B}\cdot\mathbf{n}_i$. The spin size $S=1/2$ can be absorbed by various redefinitions of the physical constants and are not shown from here on. Our notation is such that $\langle ij\rangle$ refers to the nearest-neighbor (NN) bond, and $j\in i$ refers to the summation over the (four) NN sites j that surround the site i. The mean-field spin configuration has already been laid out in Eq. (2.3), and we need to complete the orthonormal triad as

$$\begin{aligned}\mathbf{n}_i&=-n_1(-1)^i\hat{a}+n_0\hat{z},\\ \boldsymbol{\theta}_i&=n_1(-1)^i\hat{z}+n_0\hat{a},\\ \boldsymbol{\phi}_i&=\hat{b}.\end{aligned} \tag{2.10}$$

This choice of parametrizing the triad is convenient because several terms in the Hamiltonian (3.8) vanish automatically: $\boldsymbol{\theta}_i\times\boldsymbol{\theta}_j=\mathbf{0}$, and $\boldsymbol{\theta}_i\cdot\boldsymbol{\phi}_j=\boldsymbol{\phi}_i\cdot\boldsymbol{\theta}_j=0$. Remaining terms are $\boldsymbol{\theta}_i\cdot\boldsymbol{\theta}_j=-1$, $\boldsymbol{\phi}_i\cdot\boldsymbol{\phi}_j=\cos 2\theta_c=-\mathbf{n}_i\cdot\mathbf{n}_j$, $\mathbf{D}_{ij}\cdot\boldsymbol{\phi}_i\times\boldsymbol{\phi}_j=J\sin 2\theta_c\tan 2\theta_c$ for both $j=i+\hat{x}$ and $j=i+\hat{y}$, and $\mathbf{D}_{ij}\cdot\boldsymbol{\theta}_i\times\boldsymbol{\phi}_j=\mathbf{D}_{ij}\cdot\boldsymbol{\phi}_i\times\boldsymbol{\theta}_j=\pm n_1D(\cos\theta_d+\sin\theta_d)$. The $\pm$ signs refer to $j=i+\hat{x}$ and $j=i+\hat{y}$, respectively. The magnon Hamiltonian in real space becomes

$$\begin{aligned}H=&(4J'S+Bn_0)\textstyle\sum_i b_i^\dagger b_i-J\sum_{\langle ij\rangle}t_i^\theta t_j^\theta+J'\sum_{\langle ij\rangle}t_i^\phi t_j^\phi\\ &+D'\textstyle\sum_i\left(t_i^\theta t_{i+\hat{x}}^\phi+t_i^\phi t_{i+\hat{x}}^\theta\right)-D'\sum_i\left(t_i^\theta t_{i+\hat{y}}^\phi+t_i^\phi t_{i+\hat{y}}^\theta\right),\end{aligned} \tag{2.11}$$

where $J'=J/\cos 2\theta_c$ and $D'=n_1D(\cos\theta_d+\sin\theta_d)$. The magnon Hamiltonian in momentum space is

$$H=\frac{1}{2}\sum_k\psi_k^\dagger H_k^0\psi_k, \tag{2.12}$$

where

$$\begin{aligned}\psi_k&=\begin{pmatrix}b_k\\ b_{-k}^\dagger\end{pmatrix},\ H_k^0=\begin{pmatrix}A_k & B_k\\ B_k^* & A_k\end{pmatrix},\\ A_k&=4J'+Bn_0+(J'-J)(\cos k_x+\cos k_y),\\ B_k&=-(J'+J)(\cos k_x+\cos k_y)-2iD'(\cos k_x-\cos k_y).\end{aligned} \tag{2.13}$$

Using the abbreviations $X=\cos k_x$ and $Y=\cos k_y$, we obtain the magnon energy spectrum

$$E_k=\sqrt{A_k^2-|B_k|^2}=\sqrt{[4J'-2J(X+Y)+Bn_0][2J'(2+X+Y)+Bn_0]-(2D')^2(X-Y)^2}. \tag{2.14}$$

The spectrum has two local minima, at $k=0$ and $k=Q=(\pi,\pi)$, with the minimum energy at $k=0$ given by

$$E_0=\sqrt{(4(J'-J)+Bn_0][8J'+Bn_0]}. \tag{2.15}$$

It is governed by the larger of the DM energy, $J'-J\sim D^2/J$, and the Zeeman energy Bn_0. Spin-rotation invariance of the Hamiltonian is completely lost due to the DM vector, and one sees a magnon gap of order D^2/J even in the absence of the Zeeman field.

The magnon spectrum derived from the Hamiltonian (2.1) is well-known [30], but little attention has been paid to the magnon eigenstates and the associated Berry curvature. The magnon eigenstate is given in the spinor form as follows:

$$\begin{aligned}|\psi_k\rangle&=\begin{pmatrix}\cosh\theta_k/2\\ -e^{-i\phi_k}\sinh\theta_k/2\end{pmatrix},\ e^{i\phi_k}=\frac{B_k}{|B_k|},\\ \cosh\frac{\theta_k}{2}&=\sqrt{\frac{A_k}{2E_k}+\frac{1}{2}},\ \sinh\frac{\theta_k}{2}=\sqrt{\frac{A_k}{2E_k}-\frac{1}{2}}.\end{aligned} \tag{2.16}$$

Transformation to the quasiparticle operator γ_k is implemented by the formula

$$b_k=\cosh\frac{\theta_k}{2}\gamma_k-e^{i\phi_k}\sinh\frac{\theta_k}{2}\gamma_{-k}^\dagger. \tag{2.17}$$

The Berry curvature of the magnon band can be calculated exactly [9] as ($\partial_\mu=\partial/\partial k_\mu$, $\sigma_3=$ the Pauli matrix)

$$\begin{aligned}\mathcal{B}_k&=i\langle\partial_x\psi_k|\sigma_3|\partial_y\psi_k\rangle-i\langle\partial_y\psi_k|\sigma_3|\partial_x\psi_k\rangle\\ &=\frac{1}{2}\sinh\theta_k(\partial_x\phi_k\partial_y\theta_k-\partial_y\phi_k\partial_x\theta_k)\\ &=2D'(J'+J)(4J'+Bn_0)\frac{\sin k_x\sin k_y}{E_k^3}.\end{aligned} \tag{2.18}$$

The proportionality $\mathcal{B}_k\propto D'$ implies that the Berry curvature is possible only by the DM interaction. In the vicinity of $k=0$, one can write approximately

$$\mathcal{B}_k\approx\frac{16D'J^2}{E_0^3}k_xk_y, \tag{2.19}$$

which highlights the d_{xy} character in the curvature function.

The thermal Hall conductivity κ_{xy} is deduced from the Berry curvature through the formula developed by Murakami and collaborators [9,10]:

$$\frac{\kappa_{xy}}{T}=-\frac{k_B^2}{\hbar}\int\frac{d^2k}{(2\pi)^2}\left(c_2(E_k)-\frac{\pi^2}{3}\right)\mathcal{B}_k, \tag{2.20}$$

where $c_2(E_k)$ is some generalized Bose-Einstein distribution function of magnons. We find $\kappa_{xy}=0$ by symmetry of the integral in Eq. (2.20). Specifically, $\mathcal{B}_k$ changes sign under either $k_x\to -k_x$ or $k_y\to -k_y$, but E_k does not.

III. LOCAL DEFECT SCENARIO

A. Local spirals

In a series of papers, Sushkov and collaborators have argued that holes introduced by a doping Sr atom at the La site, for instance, get localized and distort the local spin configuration into a spiral with the wave vector $K = \sqrt{2}x(\pi, -\pi)$ for a given doping concentration $0 < x \lesssim 0.055$ [31–33]. For $0.055 \lesssim x \lesssim 0.12$ the K vector is directed along the crystallographic axis in accordance with the stripe scenario: $K = 2x(\pm\pi, 0)$.

Inspired by this proposal, we generalize the ground-state triad (2.10) to incorporate the spiral structure by writing

$$\begin{aligned} \mathbf{n}_i &= n_1(-1)^i \hat{a}_i - n_0 \hat{z}, \\ \boldsymbol{\theta}_i &= (-1)^i \hat{b}_i, \\ \boldsymbol{\phi}_i &= n_0(-1)^i \hat{a}_i + n_1 \hat{z}, \end{aligned} \tag{3.1}$$

where the local orthonormal vectors $\hat{a}_i$ and $\hat{b}_i$ are now position dependent:

$$\begin{aligned} \hat{a}_i &= \hat{a}\cos\theta_i + \hat{b}\sin\theta_i, \\ \hat{b}_i &= \hat{b}\cos\theta_i - \hat{a}\sin\theta_i. \end{aligned} \tag{3.2}$$

Having $\theta_i = 0$ irrespective of site i corresponds to the magnetic order considered previously. Having $\theta_i = K \cdot r_i$ with $|K| \ll 1$ corresponds to the uniform spiral of slow modulation. Sushkov's scenario corresponds to having a finite rotation angle θ_i only in the vicinity of the impurity site. We first consider the uniform spiral and the effect it has on the magnon Hall effect. Local spiral scenario will be considered subsequently.

There is an immediate consequence of having a finite spiral rotation angle θ_i. The inner products $\boldsymbol{\theta}_i \cdot \boldsymbol{\phi}_j$ and $\boldsymbol{\phi}_i \cdot \boldsymbol{\theta}_j$, previously equal to zero in the general magnon Hamiltonian (3.8), are now finite:

$$\boldsymbol{\theta}_i \cdot \boldsymbol{\phi}_j = n_0 \sin(\theta_i - \theta_j) = -\boldsymbol{\phi}_i \cdot \boldsymbol{\theta}_j. \tag{3.3}$$

Note that this term is nonzero only if the uniform moment n_0 is present simultaneously. As a consequence, the Hamiltonian matrix H_k^0 in Eqs. (2.12) and (2.13) is modified to $H_k^0 + H_k^1$, where

$$H_k^1 = -2Jn_0(\sin K_x \sin k_x + \sin K_y \sin k_y)\sigma_3. \tag{3.4}$$

This new piece of Hamiltonian creates a simple shift in the magnon spectrum $E_k \to E_k + \delta E_k$:

$$\delta E_k = -2Jn_0(\sin K_x \sin k_x + \sin K_y \sin k_y). \tag{3.5}$$

This is reminiscent of the Doppler shift; magnons whose momentum is parallel (antiparallel) to $K = (K_x, K_y)$ experience a red-shift (blue-shift) in energy.

Meanwhile, the magnon wave function (2.16) and the Berry curvature (2.18) obtained earlier remain unchanged. In particular the various energy factors in the wave function and the Berry curvature are still those of the unperturbed Hamiltonian, maintaining the symmetries $E(k_x, -k_y) = E(-k_x, k_y) = E(k_x, k_y)$. The new magnon energy $E_k + \delta E_k$ enters solely through the distribution function $c_2(E_k + \delta E_k)$ of the thermal Hall conductivity formula (2.20), which undergoes the correction

$$\begin{aligned} \delta\kappa_{xy} &\propto \sum_k \frac{\partial c_2[E_k]}{\partial E_k} \mathcal{B}_k \delta E_k \\ &\propto \sum_k \frac{\partial c_2[E_k]}{\partial E_k} \mathcal{B}_k (\sin K_x \sin k_x + \sin K_y \sin k_y) = 0. \end{aligned} \tag{3.6}$$

The first two terms in the sum, $\partial c_2/\partial E_k$ and B_k, are even under the change $k \to -k$, while δE_k is odd. As a result, the sum must be zero. The uniform spiral state fails to produce the Hall effect.

Akin to the original Sushkov proposal, we now look into the influence of localized spirals on the thermal Hall transport of magnons. First of all, we lay down some general strategy for attacking such a problem. The continuum language is more appropriate for dealing with problems that break the translation symmetry, and we begin with a continuum form of the Hamiltonian H_1 introduced in Eq. (3.4):

$$\begin{aligned} H_1 &= iJn_0 \sum_{\langle ij \rangle} \sin(\theta_i - \theta_j)(b_j^\dagger b_i - b_i^\dagger b_j) \\ &\to iJn_0 \int_r \nabla\theta (b^\dagger \nabla b - b \nabla b^\dagger). \end{aligned} \tag{3.7}$$

The integral symbol $\int_r = \int dxdy$ is abbreviated. Spatial gradient of the phase $\nabla\theta$ is localized around the impurity site. The solution worked out by Sushkov *et al.* [31–33] gives

$$\theta_\alpha = f(|r - r_\alpha|)\hat{b} \cdot (r - r_\alpha), \tag{3.8}$$

around each impurity centered at r_α. For a collection of impurities the phase twist is the sum $\theta = \sum_\alpha \theta_\alpha$. The envelope function $f(r)$ approaches the constant f_0 at the center of impurity and produces a spiral-like configuration locally.

At the level of Born scattering, the perturbation H_1 fails to produce any Hall-like transport of magnons. To see this, one writes H_1 in Fourier space,

$$H_1 = -iJSn_0 \sum_{k,p} p(p + 2k)\theta_p b_{k+p}^\dagger b_k, \tag{3.9}$$

where θ_p is the Fourier transform of the real space θ. The Born scattering amplitude $\langle k + p|H_1|k\rangle$ is proportional to the factor $p(p + 2k) = (k + p)^2 - k^2$. Under the continuum approximation, however, the quasiparticle energy E_k is a quadratic function of k [see Eq. (2.14) for the full energy dispersion]. The elastic scattering process satisfies $E_{k+p} = E_k$; hence $(k + p)^2 - k^2 = 0$. The Born scattering amplitude vanishes. Higher-order contributions from H_1 involve higher powers of the uniform moment n_0 and are expected to give a negligible contribution.

Upon expanding to one higher order in the phase gradient, we do find an additional correction in the form

$$H_2 \approx \frac{1}{4} JS \sum_r (\nabla\theta)^2 (b^\dagger - b)^2. \tag{3.10}$$

The Born scattering calculation based on this Hamiltonian also gives negative results for the magnon Hall effect. Details are not illuminating and are omitted here.

B. Local skyrmions

Speculations of skyrmion formulation in the cuprates have been around for a long time [34–36] and revived recently with the report of their sightings in a member of the cuprate family, $La_2Cu_{0.97}Li_{0.03}O_4$ [37]. It has been well-established in the recent skyrmion literature that a magnon sees a localized skyrmion as two units of flux quanta [11,38–41] and will experience Aharonov-Bohm scattering. We examine whether such a scenario can apply to the antiferromagnetic skyrmions, assuming they do form localized defects in the underdoped or undoped cuprates.

In a nutshell, an antiferromagnetic skyrmion *per se* does not give rise to the magnon Hall effect, although the ferromagnetic skyrmion does. The difference can be outlined most simply in the continuum field theory of magnons for each case. For the ferromagnetic model we switch $J \to -J$ in the magnon Hamiltonian and treat $\mathbf{n}_i$, $\boldsymbol{\theta}_i$, and $\boldsymbol{\phi}_i$ as smooth functions of the coordinates, as there is no staggered component in any of them. The continuum limit of the magnon Hamiltonian with $\mathbf{D}_{ij} = 0$ and $\mathbf{B} = 0$ is easily obtained as

$$H_{\rm FM} \sim -\frac{J}{2}\sum_\mu b^\dagger[\partial_\mu - ia_\mu]^2 b + \cdots, \tag{3.11}$$

where the curl of the vector potential $\partial_x a_y - \partial_y a_x = (2\pi)^{-1}\mathbf{n}\cdot(\partial_x \mathbf{n}\times\partial_y\mathbf{n})$ represents the local skyrmion density. The integral of the curl $(\boldsymbol{\nabla}\times\mathbf{a})_z$ is -2 for a skyrmion charge of -1. This is the basis of the claim that the local skyrmion magnetic structure acts as two units of flux quanta for the magnons. The magnon Hall effect due to skyrmions has been observed experimentally in ferromagnetic thin films [13].

A very different effective theory of magnons is found for antiferromagnetic ground states. The smooth texture is realized for the *staggered magnetization*, so the ground-state triad is parametrized as

$$\mathbf{n}_i \to (-1)^i \mathbf{n}_i^s, \quad \boldsymbol{\theta}_i \to (-1)^i \boldsymbol{\theta}_i^s, \quad \boldsymbol{\phi}_i \to \boldsymbol{\phi}_i. \tag{3.12}$$

Both $\mathbf{n}_i$ and $\boldsymbol{\theta}_i$ are staggered but not $\boldsymbol{\phi}_i$, which is defined as the cross product $\boldsymbol{\phi}_i = \mathbf{n}_i \times \boldsymbol{\theta}_i$. Now treating $\mathbf{n}_i^s$, $\boldsymbol{\theta}_i^s$, and $\boldsymbol{\phi}_i$ as smooth, we obtain the continuum magnon Hamiltonian

$$H_{\rm AFM} = \frac{J}{2}\sum_\mu [(\partial_\mu b^\dagger)^2 + (\partial_\mu b)^2] + \cdots. \tag{3.13}$$

Various other terms proportional to b^2, $(b^\dagger)^2$, and $bb^\dagger$ are not shown. Crucially, there is no analog of the covariant derivative $\partial_\mu - ia_\mu$ in this theory and no source of the emergent magnetic field. The magnon Hall effect originating from the skyrmion spin texture must be absent in the antiferromagnetic ground state.

As we saw earlier, however, undoped cuprate is weakly ferrimagnetic, due to the DM interaction and the consequent canting of spins. Since a ferrimagnet has characteristics of both ferromagnets and antiferromagnets, we find it worth exploring possible low-energy magnon dynamics for a ferrimagnetic spin-textured ground state. To this end one needs a more elaborate setup for treating magnon dynamics by allowing the triad of orthonormal vectors $(\mathbf{n}_i, \boldsymbol{\theta}_i, \boldsymbol{\phi}_i)$ to carry both staggered and uniform components locally:

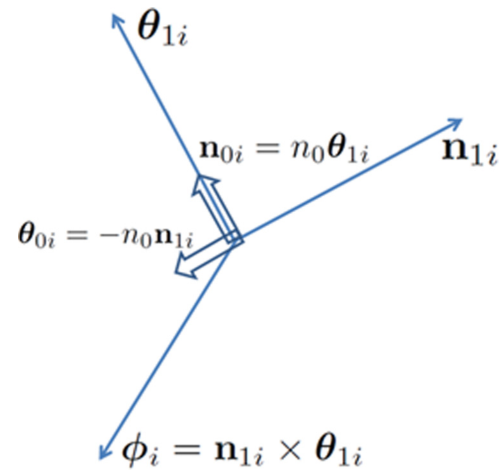

FIG. 1. Coordinate system used in developing the magnon dynamics of the ferrimagnetic ground state.

$$\begin{aligned}\mathbf{n}_i &= (-1)^i \mathbf{n}_{1i} + n_0 \boldsymbol{\theta}_{1i},\\ \boldsymbol{\theta}_i &= (-1)^i \boldsymbol{\theta}_{1i} - n_0 \mathbf{n}_{1i},\\ \boldsymbol{\phi}_i &= \mathbf{n}_{1i}\times\boldsymbol{\theta}_{1i}.\end{aligned} \tag{3.14}$$

Words of explanation are in order for this choice of parametrization. The uniform moment $\mathbf{n}_{0i}$ is by assumption orthogonal to the staggered moment $\mathbf{n}_{1i}$. The staggered component of $\boldsymbol{\theta}_i$, denoted $\boldsymbol{\theta}_{1i}$, is also orthogonal to $\mathbf{n}_{1i}$. Since both $\mathbf{n}_{0i}$ and $\boldsymbol{\theta}_i$ are required to be orthogonal to $\mathbf{n}_{1i}$, and there is a U(1) degree of freedom in choosing the orthonormal vector $\boldsymbol{\theta}_{1i}$, we invoke this freedom to choose $\boldsymbol{\theta}_{1i}$ to be parallel to $\mathbf{n}_{0i}$ or write $\mathbf{n}_{0i} = n_0\boldsymbol{\theta}_{1i}$. This explains the parametrization of $\mathbf{n}_i$ in the first line of Eq. (3.14). The second line for $\boldsymbol{\theta}_i$ follows naturally from requiring $\mathbf{n}_i \cdot \boldsymbol{\theta}_i = 0$. Orthogonality of all three vectors in Eq. (3.14) is ensured up to first order in the small moment n_0. The parametrization we propose is summed up pictorially in Fig. 1.

Substituting Eq. (3.14) into the general magnon Hamiltonian (3.8) yields the following terms, linear in n_0:

$$\begin{aligned}\boldsymbol{\theta}_i\cdot\boldsymbol{\phi}_j &\approx -n_0\mathbf{n}_{1i}\cdot(\mathbf{n}_{1j}\times\boldsymbol{\theta}_{1j}) \to -\mathbf{n}_0\cdot(\mathbf{n}_1\times\partial_\mu\mathbf{n}_1),\\ \boldsymbol{\phi}_i\cdot\boldsymbol{\theta}_j &\approx -n_0\mathbf{n}_{1i}\times\boldsymbol{\theta}_{1i}\cdot\mathbf{n}_{1j} \to \mathbf{n}_0\cdot(\mathbf{n}_1\times\partial_\mu\mathbf{n}_1).\end{aligned} \tag{3.15}$$

In arriving at the expressions at the far right we assumed a continuum approximation and introduced ∂_μ for the spatial derivative in the direction $j = i + \hat{\mu}$. A new contribution to the magnon dynamics arises from

$$\begin{aligned}H_1 &= iJ\sum_{\mu=x,y}\int dxdy(\mathbf{n}_0\cdot\mathbf{n}_1\times\partial_\mu\mathbf{n}_1)(b^\dagger\partial_\mu b - b\partial_\mu b^\dagger)\\ &= J\sum_{\mu=x,y}\int dxdy(\mathbf{a}\cdot\mathbf{j}),\end{aligned} \tag{3.16}$$

where the vector potential $\mathbf{a}$ and the magnon current density $\mathbf{j}$ are defined by $a_\mu = -\mathbf{n}_0\cdot\mathbf{n}_1\times\partial_\mu\mathbf{n}_1$ and $j_\mu = -i(b^\dagger\partial_\mu b - b\partial_\mu b^\dagger)$, respectively.

For the nontextured ground state, the uniform and staggered moments are related by $\mathbf{n}_0 = n_0\hat{b}\times\mathbf{n}_1$ through the DM interaction. If we assume that this relation continues to hold even for the textured spin configuration such as that of a skyrmion, it turns out one can write the vector potential in a much simpler form: $\mathbf{a} = -n_0 \nabla(\hat{b} \cdot \mathbf{n}_1)$. In this case, the Hamiltonian H_1 reduces exactly to the form $H_1 \sim J n_0 \nabla\theta \cdot \mathbf{j}$ we discussed in the earlier subsection. The Born scattering amplitude there was zero, and so is it here. To conclude, even the ferrimagnetic skyrmion scenario fails to produce skew scattering at the level of Born scattering. Again, more elaborate theories are likely to involve higher powers of n_0 and very small effects.

All of the local defect scenarios considered in this section fail to show skew scattering, at least at the lowest order in the uniform moment n_0. There is also a general issue of how to reconcile the impurity-induced defects with the undoped cuprate, where the impurities are nominally absent. Finally, the magnon gap grows with the magnetic field and suppresses the response function in any magnon-based scenarios. The experiment on κ_{xy} does not show such activation behavior [23].

IV. FERMIONIC SPINON THEORY OF THERMAL HALL EFFECT

With the general inability of the magnon theory to account for the observed thermal Hall effect in the undoped to lightly doped cuprates, we look for an alternative theory. A very natural candidate is to assume the existence of spinon excitations. There are many different classes of spinon models [42]. Within the context of the cuprates, a common starting point is the so-called π-flux phase, where there is π flux per plaquette resulting in fermion spinons with a Dirac dispersion at $(\pi/2, \pi/2)$ and symmetry-related points. It is then assumed that, due to strong gauge field fluctuations, the spinons are bound in a confined phase and antiferromagnetism appears, so that the only low-energy fluctuations are $S = 1$ spin waves (for a review see Ref. [43]) The spinon idea has been adopted also to compute spin dynamics in the undoped cuprates [25,26], even though long-range magnetic ordering in such compound has been well established. The spinon-based theories were rationalized by the fact that some aspects of high-energy spin excitations are not captured by the spin-wave picture alone and that a vestige of spinon excitations must remain in the physical spectrum to account for the spin dynamics fully. However, the expectation has been that the spinon gap is relative large (a fraction of J) and that the confined spinons will not influence low-temperature properties. Hence the spinon-based theories have not been applied to low-energy transport properties such as the thermal Hall conduction. The recent experiment, taken at its face value, calls for a reevaluation of this traditional view.

Historically the spinons are discussed in the context of the spin-liquid state, where there is no antiferromagnetic order. However, it has been pointed out that this restriction is unnecessary, and there is a possibility of spinon excitations coexisting with antiferromagnetic (AF) order and spin waves. Such a state possesses topological order and has been called AF*. This scenario was first proposed by Balents, Fisher, and Nayak [44] and have been further discussed by Senthil and Fisher [45]. They started with a d-wave superconductor which they disordered by proliferating hc/e vortices while the $hc/2e$ vortices remained gapped. The resulting state is called a nodal spin liquid with Dirac spinons that grew out of the d-wave Bogoliubov quasiparticles. This state can coexist with antiferromagnetism at wave vector (π, π). If the nodes are connected by the AF wave vector, they will be gapped. On the other hand, if their separation is not (π, π), they may remain as gapless Dirac fermions. Guided by this line of thinking, it seems to us that the next step is to start with a Dirac spectrum given by the π-flux model and simply assume that it coexists with the antiferromagnetism.

We proceed to first present a simple spinon-based model of magnetic dynamics and use it to compute the thermal Hall conductivity and the spin chirality. Our goal is to find the simplest model that can give results that are qualitatively similar to the observed thermal Hall effect. Even this is a highly nontrivial task because the experiment imposes serious constraints. First, as we shall see, the observed κ_{xy}^{2D}/T is very large when expressed in the natural unit of $k_B^2/\hbar$ per layer. Second, the effect is seen down to quite low temperatures of about 5 K, which says that the spinon gap cannot be too large. Third, the effect is linear in B. This rules out chiral spin-liquid states which spontaneously break the time-reversal symmetry and which will lead to hysteretic behavior that is not seen experimentally. While the Dirac nodes have Berry curvatures near the nodes, they are canceled between two sets of nodes and by themselves will not give rise to the thermal Hall effect. Thus we need to introduce some chirality which is induced linearly with the applied magnetic field. There are two ways an external field couples to the spinons. First is via the Zeeman effect and the second is a coupling to the spin chirality, As we discuss later, this latter coupling is proportional to the flux generated by the external field per plaquette and is extremely small. Therefore we considered the Zeeman coupling only and we came up with the model discussed below. We do not think this model is realistic for the cuprates. We assume a spin-dependent hopping which is possible only in the presence of spin-orbit coupling, which is not believed to be strong for the cuprates. At this stage of the development, we believe there is value in this exercise, if only to emphasize the challenge we face in coming up with even a phenomenological model that satisfies the experimental constraint outlined above.

We outline general requirements in a candidate spinon model. First, it will consist of spin-up and spin-down fermion bands with identical dispersions and opposite Berry curvatures. As such, the Hall effect of one species of fermions will be canceled out by that of the other. The applied magnetic field will then split the energy degeneracy and lead to the noncancellation of Berry curvatures, resulting in nonzero thermal Hall conductivity. In such a picture, the predicted Hall signal will be naturally proportional to the field strength B: $\kappa_{xy} \propto B$—a prominent feature in the observed thermal Hall effect in underdoped cuprates [23].

The model we present can be summed up as a 2×2 fermion Hamiltonian:

$$H = \frac{1}{2} \sum_{k\sigma} \psi_{k\sigma}^{\dagger} H_{k\sigma} \psi_{k\sigma}. \tag{4.1}$$

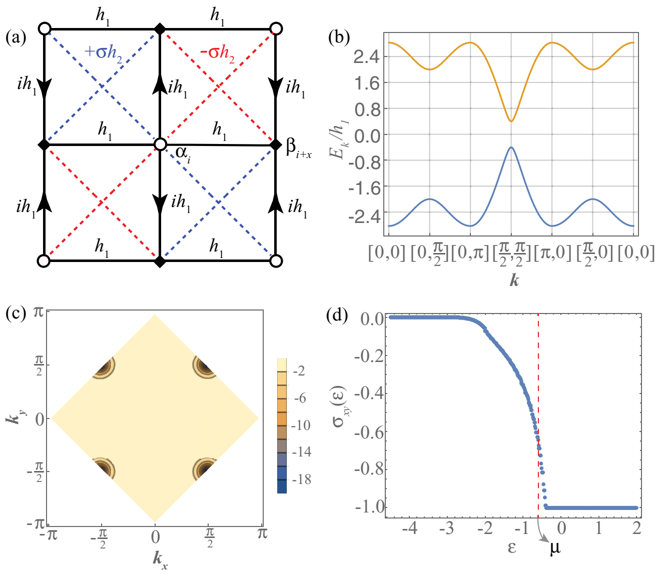

FIG. 2. (a) Hopping parameters adopted in our fermion model. Arrows indicate the imaginary hopping direction. The sign of the diagonal hopping depends on spin $\sigma = \pm 1$. (b) Upper- and lower-band dispersions obtained from the spinon model. (c) Berry curvature of the lower band over the Brillouin zone. (d) Hall conductivity $\sigma_{xy}(\epsilon)$. States with $\epsilon < \mu$ are occupied at zero temperature. Plots are drawn with $h_1 = 1$ and $h_2 = 0.1$.

For each spin $\sigma = \uparrow, \downarrow$ we have the spinor $\psi_{k\sigma} = \binom{\alpha_{k\sigma}}{\beta_{k\sigma}}$ and the Hamiltonian matrix

$$H_{k\sigma} = \begin{pmatrix} 4\sigma h_2 s_x s_y - \sigma B & 2h_1(c_x + ic_y) \\ 2h_1(c_x - ic_y) & -4\sigma h_2 s_x s_y - \sigma B \end{pmatrix}. \quad (4.2)$$

We have used the abbreviations $c_{x(y)} = \cos k_{x(y)}$ and $s_{x(y)} = \sin k_{x(y)}$. The hopping amplitudes in the nearest-neighbor and the diagonal directions are as displayed in Fig. 2. Without the diagonal hopping this is the π-flux Hamiltonian whose energy spectrum has Dirac nodes [25,26]. The diagonal hopping term h_2 opens up a gap at the Dirac points and creates bands with Chern numbers. The spin-dependent diagonal hopping amplitude is designed to generate opposite signs of Berry curvature between the two spin orientations. The Zeeman energy $-\sigma B$ is included in the Hamiltonian.

Diagonalizing the Hamiltonian, we find the energy and the Berry curvature of the bands as follows:

$$E_{nk\sigma} = 2n\left[h_1^2\left(c_x^2 + c_y^2\right) + 4h_2^2 s_x^2 s_y^2\right]^{1/2} - \sigma B,$$
$$\mathcal{B}_{nk\sigma} = 2n\sigma \frac{h_1^2 h_2\left(1 - c_x^2 c_y^2\right)}{\left[h_1^2\left(c_x^2 + c_y^2\right) + 4h_2^2 s_x^2 s_y^2\right]^{3/2}}. \quad (4.3)$$

The band index $n = \pm 1$ refers to the upper band and the lower band, respectively. The Berry curvature $\mathcal{B}_{nk\sigma}$ has opposite signs between the two bands and between the two spins. For visualization of the band dispersion and the Berry curvature, see Fig. 2. The upper and lower bands are separated by a gap of magnitude $8|h_2|$ at $(k_x, k_y) = (\pm\pi/2, \pm\pi/2)$.

The zero-temperature Hall conductivity at the putative chemical potential ϵ for each spin species is derived from the Berry curvature through the TKNN formula [1]

$$\sigma_{xy\sigma}(\epsilon) = \textstyle\sum_{nk} \mathcal{B}_{nk\sigma}\theta(\epsilon - E_{nk\sigma}), \quad (4.4)$$

which involves the sum over all states whose energies lie below ϵ. In the quantized case we obtain $\sigma_{xy} = C/2\pi$, where C is the Chern number. The lower band in our fermion model has the spin-dependent Chern number $C_\sigma = -\sigma$ for $\sigma = \pm 1$ $(\uparrow, \downarrow)$. For calculation of the thermal conductivity in the fermionic model we use the formula derived in Ref. [46]:

$$\frac{\kappa_{xy}^{2D}}{T} = \frac{1}{4T^3}\int d\epsilon \frac{(\epsilon - \mu)^2}{\cosh^2[\beta(\epsilon - \mu)/2]}\sigma_{xy}^{\rm tot}(\epsilon). \quad (4.5)$$

This has the form of a well-known Mott formula relating the thermal conductivity to the electric conductivity. To restore physical units to the dimensionless form of κ_{xy}^{2D}/T given above, one has to multiply by $k_B^2/\hbar$, the ratio of Boltzmann's constant and the Planck's constant. It is useful to note that $k_B^2/\hbar = 1.81 \times 10^{-12}$ W/K^2. As an example, consider a bulk La_2CuO_4 sample whose c-axis constant is $d = 13.2$ Å. Since there are two CuO_2 layers per unit cell, the effective interlayer distance is half that, $d_{\rm eff} = 6.6$ Å. If each CuO_2 layer carried a two-dimensional κ_{xy}^{2D}/T worth the universal value $k_B^2/\hbar$, the three-dimensional thermal Hall conductivity of the bulk La_2CuO_4 would be given by $\kappa_{xy}^{3D}/T = \kappa_{xy}^{2D}/(T d_{\rm eff}) = 2.76$ mW/K^2 m. The recently observed thermal Hall conductivity in cuprates reaches maximal κ_{xy}^{3D} values in the vicinity of 30–40 mW/K m at $T \approx 10$ K, consistent with a per layer value of κ_{xy}^{2D}/T roughly equal to $k_B^2/\hbar$ at that temperature. The thermal Hall conductivity formula (4.5) predicts values of κ_{xy}^{2D}/T in the range of $k_B^2/\hbar$ for $\sigma_{xy} \sim 1$.

The Hall conductivity $\sigma_{xy}^{\rm tot}$ itself is given as the sum of contributions from the two spin species: $\sigma_{xy}^{\rm tot}(\epsilon) = \sigma_{xy,\uparrow}(\epsilon) + \sigma_{xy,\downarrow}(\epsilon)$. In the absence of the Zeeman field we have the opposite signs of the Berry curvature and the degenerate energy bands, i.e., $\mathcal{B}_{nk\uparrow} = -\mathcal{B}_{nk\downarrow}$ and $E_{nk\uparrow} = E_{nk\downarrow}$, and hence a vanishing Hall conductivity: $\sigma_{xy,\uparrow}(\epsilon) + \sigma_{xy,\downarrow}(\epsilon) = 0$. The energy degeneracy of $\uparrow, \downarrow$-spinons are split by the Zeeman field, whereas the Berry curvature itself remains unaffected by it. The Hall conductivity formula in the presence of B becomes

$$\sigma_{xy}^{\rm tot}(\epsilon) = \sigma_{xy}(\epsilon + B) - \sigma_{xy}(\epsilon - B). \quad (4.6)$$

Here $\sigma_{xy}(\epsilon) = \sigma_{xy,\uparrow}(\epsilon)$ is the Hall conductivity of $\uparrow$-spinons. There is more occupation of $\uparrow$-spinons than $\downarrow$-spinons, because the chemical potential for the former (latter) particles has been raised (lowered) by B. In the model Hamiltonian we chose, the $\uparrow$-spinon band carries the Chern number -1 and results in negative values of κ_{xy}^{2D}.

Numerical calculations of the thermal Hall conductivity as a function of temperature and magnetic fields are shown in Fig. 3. The chemical potential was chosen in such a way that the average occupation number was $\langle f_{i\sigma}^\dagger f_{i\sigma}\rangle = n$ at zero temperature and magnetic field. The linear-B dependence of κ_{xy}^{2D}/T in the numerical plot is easy to understand, since $\sigma_{xy}(\epsilon + B) - \sigma_{xy}(\epsilon - B) \propto B$ at small values of B. Thermal smearing reduces the Hall signal at higher temperatures. The magnitude of κ_{xy}^{2D}/T values calculated within our model can reach values close to 1 ($k_B^2/\hbar$ in physical units) with suitable choices of h_2 and μ.

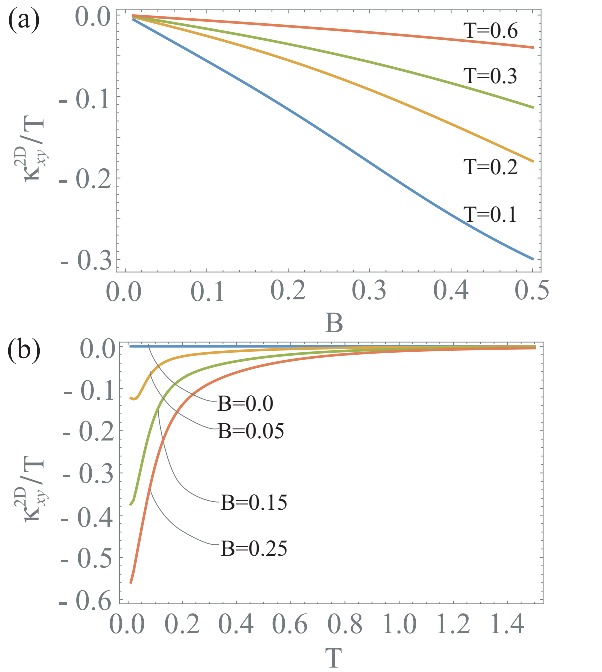

FIG. 3. Two-dimensional thermal Hall conductivity κ_{xy}^{2D}/T (in physical units of $k_B^2/\hbar$) vs (a) magnetic field B at several temperatures T and (b) vs temperature T at several magnetic fields B. Parameters chosen are $h_1 = 1$, $h_2 = 0.1$, and the chemical potential $\mu = -0.6$, corresponding to the filling factor $n = 0.98$ at $T = 0$ and $B = 0$. Temperature and magnetic field scales are measured in units of h_1.

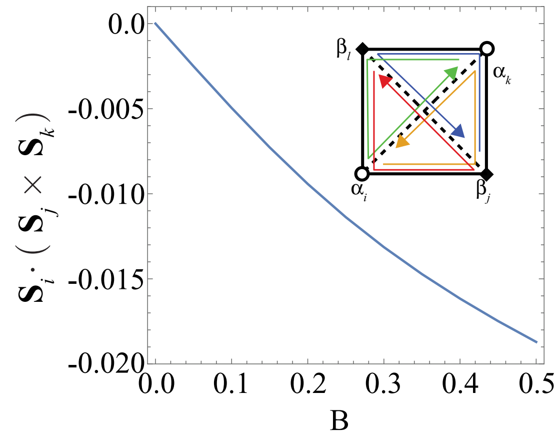

FIG. 4. Magnetic field dependence of spin chirality $\langle \mathbf{S}_i \cdot (\mathbf{S}_j \times \mathbf{S}_k)\rangle$ for the triangles of the elementary square. It grows linearly with B at small fields. Parameters used are $h_1 = 1.0$, $h_2 = 0.1$, and $\mu = -0.6$ ($n = 0.98$) as in Fig. 3. Inset: Four corners of the elementary square are labeled by i, j, k, and l. Spin chirality is calculated for each of the four triangles by going in the counterclockwise fashion. All four triangles carry the same value of spin chirality.

The spinon density n was chosen to be 0.98 in the calculation of the thermal Hall conductivity (Fig. 3). In the slave fermion model the spinon density equals the electron density on average, and at the Mott insulator limit n should be unity. In our model for $n = 1$ the thermal Hall effect is zero at zero temperature because the chemical potential will lie in the gap and the two spin species cancel. As expected based on the bulk-edge correspondence, the edge states also do not contribute even at small finite B because the up and down spins each gives a quantized κ_{xy} of opposite sign. However, it will be finite for sufficiently large B and/or temperature. The value 0.98 may be considered slightly doped. Results for other values of n are shown later.

The fermion model we study supports the spin chirality as well. In the mean-field theory, the average of the spin-chirality operator $\mathbf{S}_i \cdot (\mathbf{S}_j \times \mathbf{S}_k)$ of the $\langle ijk\rangle$ triangle becomes, through the substitution $\mathbf{S}_i = (1/2)f_i^\dagger \boldsymbol{\sigma} f_i$ with $f_i = (f_{i\uparrow}\ f_{i\downarrow})$,

$$\langle \mathbf{S}_i \cdot (\mathbf{S}_j \times \mathbf{S}_k)\rangle = -\frac{i}{2}(\chi_{ij}\chi_{jk}\chi_{ki} - \chi_{ik}\chi_{kj}\chi_{ji}), \quad (4.7)$$

where $\chi_{ij} = \sum_\sigma \langle f_{i\sigma}^\dagger f_{j\sigma}\rangle$. Calculations of χ_{ij} in the mean-field theory are straightforward. The essential point, as it turns out, is that the triple product of hopping parameters $\chi_{ijk} \equiv \chi_{ij}\chi_{jk}\chi_{ki}$ contains an imaginary term only at finite magnetic field and diagonal hopping; thus $\langle \mathbf{S}_i \cdot (\mathbf{S}_j \times \mathbf{S}_k)\rangle = \mathrm{Im}[\chi_{ijk}] \propto h_2 B$.

Explicit calculation shows all elementary triangles having the same spin chirality. In other words, a finite magnetic field induces a uniform spin chirality state within our model. Numerical evaluation of spin chiralities through the four triangles of the elementary square are shown in Fig. 4, displaying the expected linear growth with B at small fields. Our observation suggests that an interaction of the form $\sim B\mathbf{S}_i \cdot (\mathbf{S}_j \times \mathbf{S}_k)$ might be present and play a hitherto neglected role in the transport of undoped cuprates. Such an interaction Hamiltonian is well-known to derive from the large-U expansion of the Hubbard interaction, when an external magnetic field is present [47]. The application of such a spin chirality Hamiltonian to the understanding of the behavior of the spin-liquid phase under an external magnetic field was taken up in Ref. [48], where the focus was the orbital effects of the magnetic field such as the Landau level formation of spinons, without explicit consideration of the Zeeman splitting of the spinons as we do. The spinon hopping parameters in Ref. [48] pick up an imaginary part as a result of the Aharonov-Bohm effect, while our hopping parameters are deemed fixed and unchanged under the magnetic field. We also note that a spin chirality induced by a magnetic field was considered earlier by Katsura *et al.* [6] to generate a thermal Hall effect. However that effect is extrinsic, i.e., it depends on the scattering of the spinons by disorder, whereas the effect we consider in this paper is intrinsic.

Figure 5 shows the doping dependence of κ_{xy} and the spin chirality at some fixed temperature and field. As one can see, the κ_{xy}/T reaches a maximum in the vicinity of $n \approx 0.95$ in our model. The spin chirality nearly vanishes at $n = 1$, since the two orientations of spinons actually carry opposing senses of circulation, i.e., $\chi_{ij,\uparrow}\chi_{jk,\uparrow}\chi_{ki,\uparrow} \approx -\chi_{ij,\downarrow}\chi_{jk,\downarrow}\chi_{ki,\downarrow}$, and it is the residual part of their sum which contributes to the spin chirality. At $n = 1$ the cancellation is almost complete; hence the spin chirality becomes very small. Additionally, one can check that the spin-spin correlation $\langle \mathbf{S}_i \cdot \mathbf{S}_j\rangle$ preserves the lattice symmetries as well, and the loss of translational and rotational symmetry in the hopping patterns of our ansatz is only an artifact of the spinon theory. The aspect of projective symmetry restoration was discussed in Ref. [27] also.

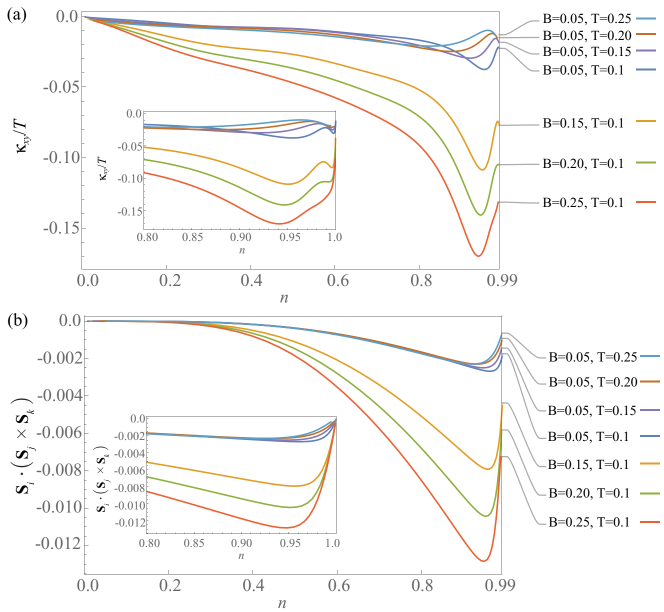

FIG. 5. Doping (n) dependence of (a) κ_{xy}/T and (b) spin chirality at several values of T and B.

The spinon model we propose is not without its drawbacks. On the theoretical side, the conventional view is that starting from a spinon model, the Néel state can emerge as a confinement transition, where the spinons become gapped and confined [43]. Thus we normally do not expect the coexistence of antiferromagnetic order and nearly free spinons. On the other hand, such coexistence is allowed but should be considered highly exotic [44,45]. Furthermore, the spinon gap must be small in the insulator in order to give a thermal Hall effect at relatively low temperature and magnetic field. The particular spinon dynamics that we assume, with spin-dependent hopping, does not have a well-defined microscopic justification at the moment, except that it might in some way be tied to spin-orbit interaction. The model on the whole is an attempt to fit the observation. On the experimental side, the renormalized spin-wave theory does a good job of accounting for the magnetic excitations in the square-lattice antiferromagnet, as revealed for instance in recent experiments [49,50]. On the other hand, some high-energy features in the magnetic excitation are not fully explained within the spin-wave theory alone [49,50], which in turn prompted speculations about residual spinon excitations in the Heisenberg model [51]. Overall it is fair to say that, at this point, spinons as low-energy excitations in square-lattice quantum antiferromagnets have quite weak experimental support. On the other hand, the two quasiparticles—magnons and spinons—give contrasting predictions in regard to their behavior under the magnetic field. In the spin-wave scenario, a magnon gap inevitably opens and suppresses the magnons' contribution to transport. For the spinon-based scenario, as demonstrated here, linear growth of the response function κ_{xy}/T with the field is natural. The diagonal spinon hopping term $\sim h_2$ necessary for the opening of the gap, the existence of Berry curvature, and ultimately the thermal Hall transport all seem closely related to the spin chirality correlation, given that the latter quantity scales with h_2 in our model. In turn, including the three-spin exchange interaction on top of the Heisenberg interaction might be a necessary ingredient for the complete understanding of magnetic dynamics in undoped cuprates.

If the spinon excitations indeed play a role in the thermal transport in the antiferromagnetic phase of the cuprates, they must have manifestations on other probes such as inelastic neutron scattering and heat capacity measurement. Calculations of such physical quantities within the same spinon scenario, coupled with critical reexamination of past experiments in light of such theory, might shed further light on the true nature of low-energy excitations in the undoped cuprates. The thermal Hall measurement on other square-lattice antiferromagnets will be a nice cross-check on the observed effect in the cuprates as well.

Note added. Spinon theory of the thermal Hall effect in magnets with Dzyaloshinskii-Moriya interaction was also advanced in a recent preprint [52] and applied to the Kagome lattice. We also mention a preprint by Chatterjee *et al.* [53] which also used the π-flux spinon as a starting point. A key ingredient is the term $J_\chi \sum_\triangle \mathbf{S}_i \cdot (\mathbf{S}_j \times \mathbf{S}_k)$ in their Eq. (2), where J_χ is proportional to the magnetic flux through a triangular plaquette. This term generates a net chirality which produces a thermal Hall effect. We considered this term in the last section but did not discuss it further because of the very small magnitude. One can make an estimate of J_χ using the t/U expansion by Motrunich [48] to find $J_\chi = -48\pi(t_2 t^2/U^2)(\phi/\phi_0)$, where $\phi_0 = hc/e = 2.07 \times 10^{-15}$ Wb is the flux quantum, and $\phi = BA_0$ is the magnetic flux through a triangular plaquette of area $A_0 \approx (3.8\ \text{Å})^2/2$ for the cuprate. At $B = 10$ T we find $\phi/\phi_0 \approx 3.5 \times 10^{-4}$. Further using commonly accepted values of $t_2 = -0.3t$, $U = 8t$, and $J = 4t^2/U$, we find $J_\chi \approx 5.6 \times 10^{-4} J$ at $B = 10$ T. The use of a smaller effective U may increase this number a bit, but in any case a very small number is expected for J_χ, due to the small ratio ϕ/ϕ_0. As we emphasized in this paper, the unexpected nature of the experimental data means that all avenues should be explored. Nevertheless, the small value of this term should be kept in mind. The assumed proximity to a quantum critical point also makes it challenging to explain the linear B dependence of κ_{xy} observed over a large range from 5 to 15 T.

ACKNOWLEDGMENTS

J.H.H. was supported by Samsung Science and Technology Foundation under Project No. SSTF-BA1701-07. P.A.L. acknowledges support by the DOE under Grant No. DE-FG02-03ER46076.

[1] D. J. Thouless, M. Kohmoto, M. P. Nightingale, and M. den Nijs, Phys. Rev. Lett. **49**, 405 (1982).
[2] F. D. M. Haldane, Phys. Rev. Lett. **61**, 2015 (1988).
[3] M. Onoda, S. Murakami, and N. Nagaosa, Phys. Rev. Lett. **93**, 083901 (2004).
[4] C. Strohm, G. L. J. A. Rikken, and P. Wyder, Phys. Rev. Lett. **95**, 155901 (2005).

[5] K. Sugii, M. Shimozawa, D. Watanabe, Y. Suzuki, M. Halim, M. Kimata, Y. Matsumoto, S. Nakatsuji, and M. Yamashita, Phys. Rev. Lett. **118**, 145902 (2017).
[6] H. Katsura, N. Nagaosa, and P. A. Lee, Phys. Rev. Lett. **104**, 066403 (2010).
[7] Y. Onose, T. Ideue, H. Katsura, Y. Shiomi, N. Nagaosa, and Y. Tokura, Science **329**, 297 (2010).
[8] T. Ideue, Y. Onose, H. Katsura, Y. Shiomi, S. Ishiwata, N. Nagaosa, and Y. Tokura, Phys. Rev. B **85**, 134411 (2012).
[9] R. Matsumoto and S. Murakami, Phys. Rev. Lett. **106**, 197202 (2011).
[10] R. Matsumoto, R. Shindou, and S. Murakami, Phys. Rev. B **89**, 054420 (2014).
[11] L. Kong and J. Zang, Phys. Rev. Lett. **111**, 067203 (2013).
[12] S.-Z. Lin, C. D. Batista, C. Reichhardt, and A. Saxena, Phys. Rev. Lett. **112**, 187203 (2014).
[13] M. Mochizuki, X. Z. Yu, S. Seki, N. Kanazawa, W. Koshibae, J. Zang, M. Mostovoy, Y. Tokura, and N. Nagaosa, Nat. Mater. **13**, 241 (2014).
[14] J. H. Han and H. Lee, J. Phys. Soc. Jpn. **86**, 011007 (2017).
[15] S. Murakami and A. Okamoto, J. Phys. Soc. Jpn. **86**, 011010 (2017).
[16] J. Romhányi, K. Penc, and R. Ganesh, Nat. Commun. **6**, 6805 (2015).
[17] M. Hirschberger, R. Chisnell, Y. S. Lee, and N. P. Ong, Phys. Rev. Lett. **115**, 106603 (2015).
[18] M. Hirschberger, J. W. Krizan, R. J. Cava, and N. P. Ong, Science **348**, 106 (2015).
[19] D. Watanabe, K. Sugii, M. Shimozawa, Y. Suzuki, T. Yajima, H. Ishikawa, Z. Hiroi, T. Shibauchi, Y. Matsuda, and M. Yamashita, Proc. Natl. Acad. Sci. USA **113**, 8653 (2016).
[20] Y. Kasahara, T. Ohnishi, Y. Mizukami, O. Tanaka, S. Ma, K. Sugii, N. Kurita, H. Tanaka, J. Nasu, Y. Motome, T. Shibauchi, and Y. Matsuda, Nature (London) **559**, 227 (2018).
[21] H. Doki, M. Akazawa, H.-Y. Lee, J. H. Han, K. Sugii, M. Shimozawa, N. Kawashima, M. Oda, H. Yoshida, and M. Yamashita, Phys. Rev. Lett. **121**, 097203 (2018).
[22] H. Lee, J. H. Han, and P. A. Lee, Phys. Rev. B **91**, 125413 (2015).
[23] G. Grissonnanche, A. Legros, S. Badoux, E. Lefrancois, V. Zatko, M. Lizaire, F. Laliberté, A. Gourgout, J.-S. Zhou, S. Pyon, T. Takayama, H. Takagi, S. Ono, N. Doiron-Leyraud, and L. Taillefer, arXiv:1901.03104.
[24] M. Kawano and C. Hotta, Phys. Rev. B **99**, 054422 (2019).
[25] T. C. Hsu, Phys. Rev. B **41**, 11379 (1990).
[26] C.-M. Ho, V. N. Muthukumar, M. Ogata, and P. W. Anderson, Phys. Rev. Lett. **86**, 1626 (2001).
[27] R. Samajdar, S. Chatterjee, S. Sachdev, and M. S. Scheurer, Phys. Rev. B **99**, 165126 (2019).
[28] T. Thio *et al.*, Phys. Rev. B **38**, 905 (1988).
[29] S.-W. Cheong, J. D. Thompson, and Z. Fisk, Phys. Rev. B **39**, 4395 (1989).
[30] D. Coffey, K. S. Bedell, and S. A. Trugman, Phys. Rev. B **42**, 6509 (1990).
[31] O. P. Sushkov and V. N. Kotov, Phys. Rev. Lett. **94**, 097005 (2005).
[32] A. Lüscher, G. Misguich, A. I. Milstein, and O. P. Sushkov, Phys. Rev. B **73**, 085122 (2006).
[33] A. Lüscher, A. I. Milstein, and O. P. Sushkov, Phys. Rev. Lett. **98**, 037001 (2007).
[34] B. I. Shraiman and E. D. Siggia, Phys. Rev. B **42**, 2485 (1990).
[35] R. J. Gooding, Phys. Rev. Lett. **66**, 2266 (1991).
[36] S. Haas, F. C. Zhang, F. Mila, and T. M. Rice, Phys. Rev. Lett. **77**, 3021 (1996).
[37] I. Raičević, D. Popović, C. Panagopoulos, L. Benfatto, M. B. Silva Neto, E. S. Choi, and T. Sasagawa, Phys. Rev. Lett. **106**, 227206 (2011).
[38] N. Nagaosa and Y. Tokura, Nat. Nanotechnol. **8**, 899 (2013).
[39] J. P. Liu, Z. Zhang, and G. Zhao, *Skyrmions: Topological Structures, Properties, and Applications* (CRC Press, Boca Raton, FL, 2016).
[40] W. Jiang, G. Chen, K. Liu, J. Zang, S. G. E. Velthuis, and A. Hoffmann, Phys. Rep. **704**, 1 (2017).
[41] J. H. Han, *Skyrmions in Condensed Matter* (Springer, Berlin, 2017).
[42] X. G. Wen, Phys. Rev. B **65**, 165113 (2002).
[43] D. Kim and P. A. Lee, Ann. Phys. **272**, 130 (1999).
[44] L. Balents, M. P. A. Fisher, and C. Nayak, Phys. Rev. B **60**, 1654 (1999).
[45] T. Senthil and M. P. A. Fisher, Phys. Rev. B **63**, 134521 (2001).
[46] T. Qin, Q. Niu, and J. Shi, Phys. Rev. Lett. **107**, 236601 (2011).
[47] D. Sen and R. Chitra, Phys. Rev. B **51**, 1922 (1995).
[48] O. I. Motrunich, Phys. Rev. B **73**, 155115 (2006).
[49] M. P. M. Dean *et al.*, Nat. Mater. **11**, 850 (2012).
[50] B. D. Piazza *et al.*, Nat. Phys. **11**, 62 (2016).
[51] H. Shao, Y. Q. Qin, S. Capponi, S. Chesi, Z. Y. Meng, and A. W. Sandvik, Phys. Rev. X **7**, 041072 (2017).
[52] Y. H. Gao and G. Chen, arXiv:1901.01522.
[53] S. Chatterjee, H. Guo, S. Sachdev, R. Samajda, M. Scheurer, N. Seiberg, and C. Xu, arXiv:1903.01992.